Supramolecular Chemistry Hot Paper

DOI: 10.1002/ange.201310485

Luminescence Enhancement after Adding Stoppers to Europium(III) Nanozeolite L**

Peng Li, Yige Wang, Huanrong Li, and Gion Calzaferri**

Abstract: *Stopper molecules attached to nanozeolite L (NZL) boost the luminescence of confined Eu^{3+}-β-diketonate complexes. The mechanism that is responsible was elucidated by comparing two diketonate ligands of different pK_a and two aromatic imines, and by applying stationary and time resolved spectroscopy. The result is that the presence of the imidazolium based stopper is favorable to the sustainable formation of Eu^{3+}-β-diketonate complexes with high coordination by decreasing the proton strength inside the channels of NZL. A consequence is that strongly luminescent transparent films can be prepared using aqueous suspension of the stopper modified composites.*

Trivalent lanthanide complexes with organic ligands have become important for a wide range of applications.[1–7] However, low thermal and photochemical stability, poor mechanical and conduction properties, as well as the tendency to aggregate severely limit their full exploitation in practical applications. A way to overcome these shortcomings is to encapsulate the complexes within the cavities of zeolites which are crystalline aluminosilicates with pores of molecular dimensions.[8–13] Wada and co-workers reported fine-tuning of the emission colors by inserting a sensitizer into the cavities of NaX zeolite co-doped with Eu^{3+} and Tb^{3+}. The emission of these composites could be tuned from violet to blue, green, and red by changing the amounts of Ln^{3+} ions and the nature of the sensitizer.[14] We and others observed considerable improvement of thermal- and photostability of lanthanide complexes when embedding them in the channels of zeolite L (ZL).[15–21] Oriented Ln^{3+} doped ZL films with tunable emission colors have been synthesized by using functional linkers that can coordinate and sensitize Ln^{3+}.[22,23]

Increasing effort has been focused on nanosized zeolite for a variety of reasons.[24–28] Embedding nanosized ZL (NZL) in polymer matrices results in transparent hybrid materials.[28–30] Films prepared with them typically exhibit high mechanical and chemical stability. A combination of the characteristics of such films with the luminescence properties of Ln^{3+} complexes is thought to be important for developing novel optical devices. Transparent films of Ln^{3+}-ZL composites prepared from colloidal suspensions exhibit weak luminescence, unfortunately. A solution of this problem could be to selectively plug the channel entrances of the ZL host by means of stopper molecules, a principle that was first communicated by Calzaferri[31] and later used and further developed in several laboratories.[32–38] Selective modification of ZL with stopper molecules can for example prevent penetration of small molecules that would otherwise enter the channels or it can prevent guests from leaving the host. It is based on the fact that ZL crystals consist of strictly one-dimensional channels. Their openings are located on the bases, causing different chemical properties with respect to the coat. Scheme 1 (A) illustrates the hexagonal channel system, (B) shows a top and a side view of the channels which have a van der Waals opening of 0.71 nm at the smallest and 1.26 nm at the widest place, and (C) shows an idealized morphology of a crystal and on the right a representation that we will use for imitating the channel structure. Scheme 1 also shows the structure of the ligands and of the stopper.

When attaching **1** to NZL, the channels of which contained $Eu^{3+}(L_n)$, we observed a very large increase of the luminescence intensity if L was a β-diketonate. This was surprising because **1** completely lacks the ability to sensitize Eu^{3+}. We further found that brightly luminescent transparent films can be prepared from aqueous suspensions of the stopper-modified composites, which we abbreviate as $Eu^{3+}(L_n)$-NZL. Details of these unexpected observations and an explanation are reported.

We choose the imidazolium salt **1** as stopper because it bears a positively charged part which easily enters the negatively charged NZL-channel upon exchanging a cation present in the neighborhood and because the bulky triethoxysilane moiety can react with the OH groups present at the channel entrances and in lower amount also at the coat. The reaction explained in Scheme 2 is similar to that reported for a triethoxysilylated coumarin.[37] The ratio of channel entrances and unit cells (u.c.) of a ZL crystal of equal length and diameter d in nm is equal to $1.485/d$. This means that for example, a 30 nm NZL consists of about 20 times more u.c. than channel entrances.[36]

[*] P. Li, Prof. Dr. Y. Wang, Prof. Dr. H. Li
School of Chemical Engineering and Technology
Hebei University of Technology
Tianjin 300130 (China)
E-mail: lihuanrong@hebut.edu.cn
Prof. Dr. G. Calzaferri
Department of Chemistry and Biochemistry, University of Bern
Freiestrasse 3, 3012 Bern (Switzerland)
E-mail: gion.calzaferri@dcb.unibe.ch

[**] Financial support by the National Key Basic Research Program (2012CB626804), the National Natural Science Foundation of China (20901022, 21171046, 21271060, and 21236001), the Tianjin Natural Science Foundation (13JCYBJC18400), the Natural Science Foundation of Hebei Province (No.B2013202243), the Program for Changjiang Scholars and Innovative Research Team in University (PCSIRT, IRT1059), and Educational Committee of Hebei Province (2011141,LJRC021) is gratefully acknowledged.

Supporting information for this article is available on the WWW under http://dx.doi.org/10.1002/anie.201310485.

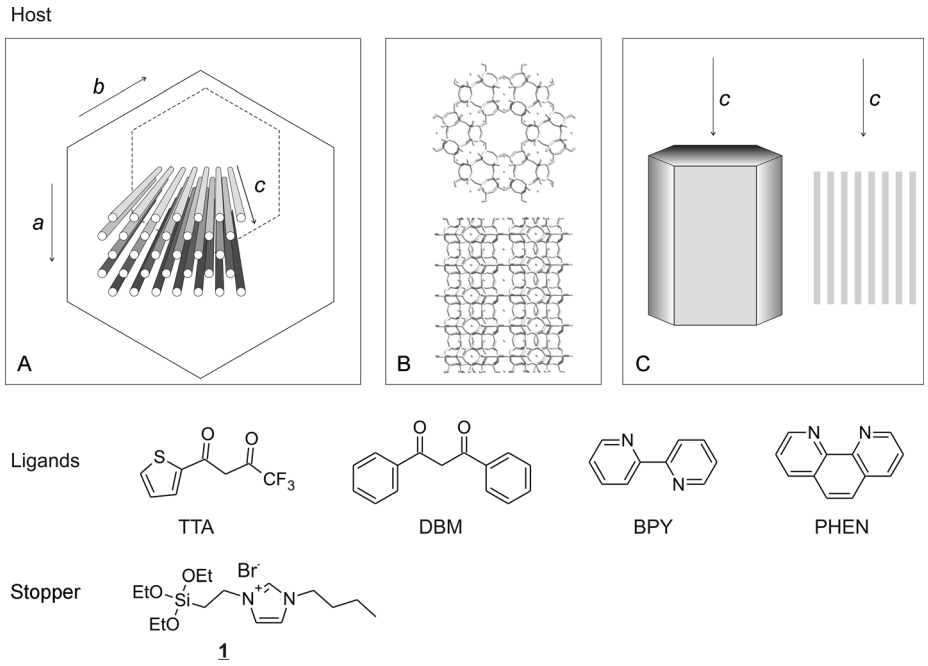

Scheme 1. Structure of the host ZL, the ligands L, and the stopper **1**.

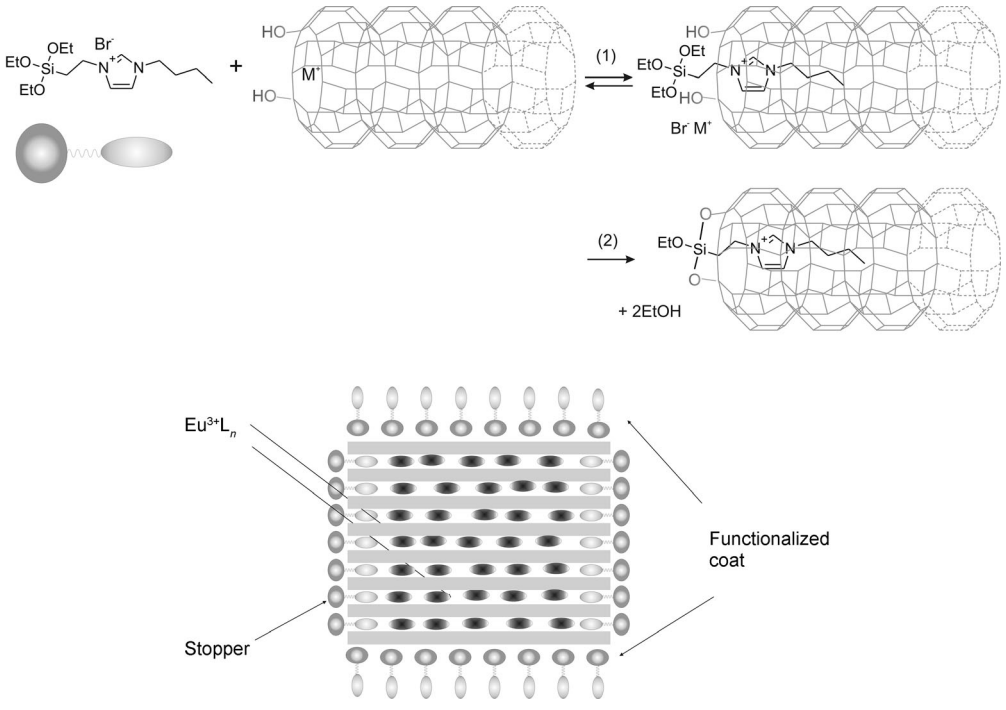

Scheme 2. Upper: selective modification of the ZL channel entrance; (1) sonication, (2) reflux. Lower: stopper and coat functionalized NZL crystal containing inside Eu^{3+} complexes as guests.

We now describe the preparation, characterization, and properties of the $Eu^{3+}(TTA_n)$-NZL and of the composites modified with **1**, which we denote as $(Eu^{3+}(TTA_n)$-NZL)-**1**(x), where x is the amount of **1** with respect to the number of channel entrances added to the modification reaction mixture. The NZL host, stopper **1**, and the $Eu^{3+}(TTA_n)$-NZL composites were prepared as described in the Supporting Information, Section S1. The experimentally determined Eu^{3+} and TTA loading of the samples were 0.66/u.c. and 3.17/u.c., respectively. Modification with **1** was carried out in aqueous environment. In the first step, the positively charged part of **1** enters the negatively charged channel by exchanging a charge compensating cation in an equilibrium reaction (Scheme 2, step 1). The $Si(OEt)_3$ part is too large to enter deep into the channel. Some **1** may also adsorbed at the coat, the amount depending on the excess present in the reaction mixture. Siloxane bonds are formed during the refluxing procedure with the OH groups present at the channel entrance (step 2), and with those present to a lesser amount at the coat of NZL.[37,38] The Eu^{3+}-(TTA_n)-NZL show remarkably enhanced luminescence, which is easily visible by eye upon near UV excitation, after this modification procedure. Figure 1 C, D shows images to give an intuitive impression of the effect. The excitation spectrum (Figure 1 A) shows a broad band ranging from 200 to 470 nm, which is assigned to the absorption of TTA.[15] The emission spectrum (Figure 1 B) displays five sharp lines at 578, 592, 612, 652, and 701 nm, ascribed to the $^5D_0 \rightarrow {}^7F_J$ ($J = 0$–4) transitions. It is dominated by the $^5D_0 \rightarrow {}^7F_2$ band at 612 nm, which is responsible for the red emission color shown in (D). This large increase of the luminescence intensity was unexpected, as **1** lacks the ability to sensitize the luminescence of Eu^{3+}. No luminescence can be observed when the Eu^{3+}-NZL is modified with **1** in absence of a sensitizing ligand.

What is the reason for this important luminescence enhancement? Additional experiments were made to find an answer to this question. FTIR spectra were used to characterize the modified materials. We checked the reactivity of **1** under the applied conditions. Its spectrum

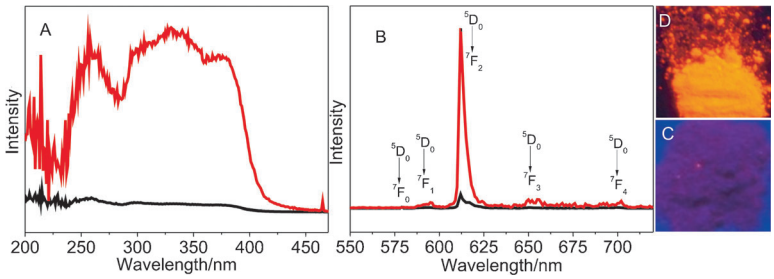

Figure 1. Excitation spectra monitored at 612 nm (A) and emission spectra (B) excited at 345 nm of $Eu^{3+}(TTA_n)$-NZL (black) and $(Eu^{3+}(TTA_n)$-NZL)-**1**(1100) (red) observed at RT. Scan slits for $Eu^{3+}(TTA_n)$-NZL and $(Eu^{3+}(TTA_n)$-NZL)-**1**(1100) were 2 and 0.3 nm, respectively. C), D): Images of the two samples taken under near UV excitation: C) $Eu^{3+}(TTA_n)$-NZL and D) $(Eu^{3+}(TTA_n)$-NZL)-**1**(1100).

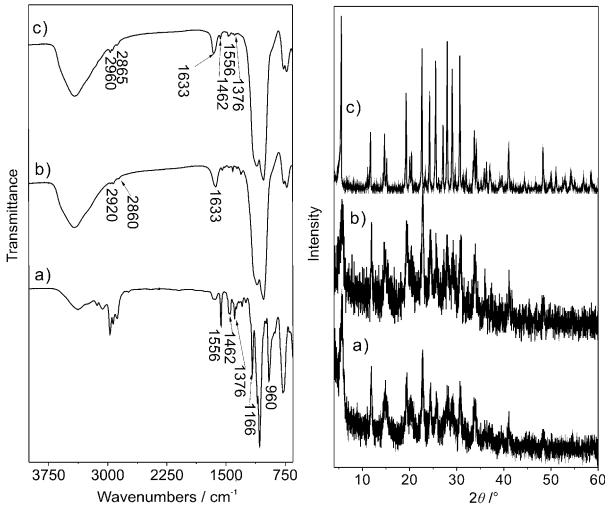

Figure 2. Left: FTIR spectra. a) **1** after sonication in water; b) $Eu^{3+}(TTA_n)$-NZL; c) $(Eu^{3+}(TTA_n)$-NZL)-**1**(1100). Right: XRD patterns. a) $Eu^{3+}(TTA_n)$-NZL; b) $(Eu^{3+}(TTA_n)$-NZL)-**1**(1100); c) ZL microcrystals.

measured after sonication in water at RT in Figure 2 (a,left) shows intense bands at 960 and 1166 cm^{-1} characteristic for the $SiOCH_2CH_3$.[39] This means that no obvious hydrolysis occurs during the sonication procedure. The bands at 1556 and 1462 cm^{-1} belong to the imidazole ring of **1**. The spectrum of $Eu^{3+}(TTA_n)$-NZL, Figure 2 (b,left) is dominated by a broad band 1160–1050 cm^{-1}, which is known to belong to the υ_{as}(T-O-T) stretching vibrations (T = Si^{4+} or Al^{3+}).[40] The water molecules are seen by the stretching and the bending modes at 3450 and 1633 cm^{-1}. The weak bands at 2920, 2860 and in the range of 1600–1400 cm^{-1} can be attributed to the TTA ligand. The presence of **1** is manifest in Figure 2 (c,left) by the characteristic imidazole ring bands at 1556 and 1462 cm^{-1}. The absence of the band at 960 cm^{-1} implies the reaction of the terminal triethoxy groups of **1** with the surface OH groups of NZL.

XRD patterns of the NZLs together with that of larger ZL crystals are shown in Figure 2 (right). The NZL exhibit the typical pattern expected for ZL with the typical line-broadening and some loss of crystallinity caused by their small size.[41] No significant changes are observed for NZL after modification with **1**, as seen by comparing Figure 2 c (right) with b (right), indicating that the modification is not detrimental to the framework.

The amount of **1** that was covalently attached to form the $(Eu^{3+}(TTA_n)$-NZL)-**1** composites was determined by elemental analysis. We found that about 1 % of the added amount x was covalently attached up to a maximum above which no further reaction took place (Figure 3; Supporting Information, Figure S3). The reaction levels off at an amount which corresponds roughly to that estimated for dense monolayer coverage. The behavior of the luminescence enhancement is similar.

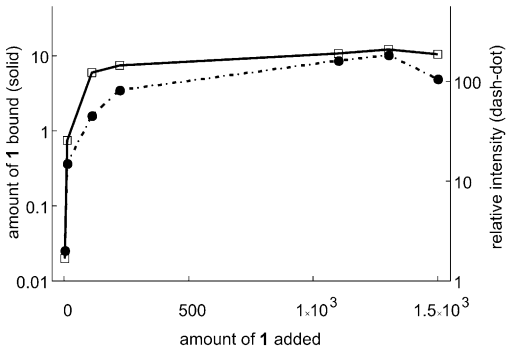

Figure 3. Amount of **1** covalently bound to the composite (solid) and luminescence intensity versus the amount x of **1** added to the reaction mixture (dash-dot). See also the Supporting Information, Figure S3.

We wondered whether this important luminescence enhancement also applies for other ligands. We therefore tested PHEN and BPY, which coordinate by the nitrogen atoms, and DBM, which is similar to TTA. The result is that the luminescence properties of $Eu^{3+}(PHEN_n)$-NZL and $Eu^{3+}(BPY_n)$-NZL are not markedly influenced by modification with **1**, in contrast to $Eu^{3+}(DBM_n)$-NZL, which shows considerable luminescence enhancement. Images of samples under near UV illumination are given in the Supporting Information, Scheme S1, and spectra of $Eu^{3+}(DBM_n)$-NZL)-**1**(x) are in Figure 4. The excitation spectra show a broad band that can be ascribed to the absorption of DBM. The emission spectra present the characteristic $^5D_0 \rightarrow {}^7F_J$ transitions, with the $^5D_0 \rightarrow {}^7F_2$ as the most prominent.

The luminescence intensity increases with increasing amount x of added **1**, which is similar to that seen in Figure 3 (Supporting Information, Figure S3) for Eu^{3+}-(TTA_n)-NZL)-**1**(x), but with lower cadence. It is known that protonation of diketonates competes with full coordination to Eu^{3+} and that incomplete coordination affects the luminescence yield. Both TTA and DBM can be protonated under the acidic environment of hydrated zeolite L, but DBM to a larger extent, as its pK_a value is larger than that of TTA, with values of 8.95 and 6.33, respectively. Following this reasoning, we find that the remarkable influence of **1** on the luminescence intensity of the β-diketonate based composites

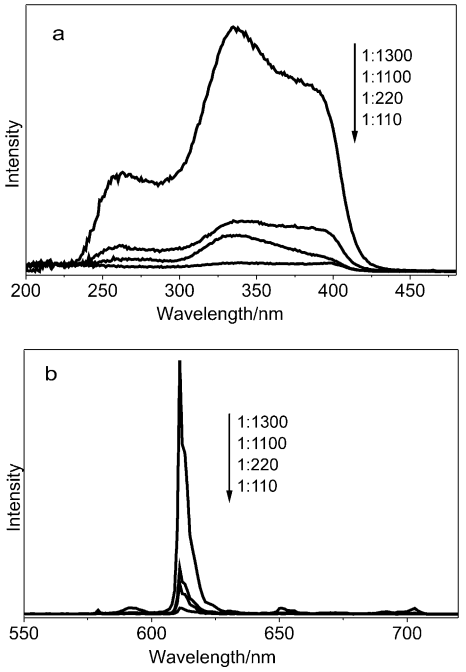

Figure 4. Excitation spectra monitored at 612 nm (a) and emission spectra excited at 350 nm (b) of $Eu^{3+}(DBM_n)$-NZL)-***1***(x), observed at RT. Luminescence of non-modified $Eu^{3+}(DBM_n)$-NZL) is too weak to be observed under the applied conditions.

Table 1: Photophysical data.

Sample	$\langle\tau\rangle$ [ms]	kr [ms^{-1}]	knr [ms^{-1}]	q [%]
$Eu^{3+}(TTA_n)$-NZL	0.09	0.9	10.21	8.1
$Eu^{3+}(TTA_n)$-NZL-**1**(1100)	0.61	1.3	0.34	79.3
$Eu^{3+}(TTA_n)$-NZL-NH_3	0.36	0.9	1.88	32.4
Film of $Eu^{3+}(TTA_n)$-NZL-**1**(1100)	0.48	1.2	0.88	57.7

are caused by a decrease of the proton activity inside of the NZL channels. Each stopper attached to the channel entrance exchanges one of the cations that control the proton strength.[42] The effect is enhanced by the fact that the imidazolium acts as a weak base.[43] This is supported by the observation illustrated in Figure 3 that very large intensity enhancement occurs at low coverage with **1** and does not increase further once a coverage of about one dense monolayer has been achieved.

Our interpretation is supported by the behavior of the intensity ratio $I(^5D_0\rightarrow{}^7F_2)/I(^5D_0\rightarrow{}^7F_1)$ and by the luminescence decay of the composites. The former increases from 13.77 to 18.97 after modification of $Eu^{3+}(TTA_n)$-NZL with **1**. Values larger than 10 are expected for Eu^{3+}-β-diketonate complexes. A value of 18.97 when encapsulated in zeolites is rarely seen, however. This intensity ratio is a measure for the asymmetry of the Eu^{3+} site. It becomes larger with increasing interaction of the Eu^{3+} with its neighbors because the site symmetry decreases.[44] We can therefore safely conclude that the large ratio observed for $Eu^{3+}(TTA_n)$-NZL-**1**(1100) reflects the lower symmetry of the Eu^{3+} site and hence a larger Eu^{3+}-ligand interaction of the modified composite which means more complete coordination to the β-diketonate. The luminescence decays shown in the Supporting Information, Figure S1 are compatible with this interpretation. They show that the excited state of the $Eu^{3+}(TTA_n)$-NZL decays much slower after modification with **1**; the luminescence decay is well represented by a bi-exponential (see the Supporting Information). The average decay time increases from 0.09 to 0.61 ms after modification. The prolonged lifetime of the Eu^{3+} excited state indicates a displacement of water molecules and/or OH groups from the first coordination sphere. We report in Table 1 the $^5D_0$ radiative (k_r) and the non-radiative (k_{nr}) rate constants, and the $^5D_0$ luminescence quantum efficiency q, as determined by the method reported in Ref. [45] in an environment of average refractive index of 1.544. The decay constants and q are consistent (Supporting Information, Figure S4).

The $Eu^{3+}(TTA_n)$-NZL-NH_3 data correspond to samples that were treated with ammonia, as a simple but only qualitative check regarding the influence of increasing pH in the channels of NZL. This exposure had a qualitatively similar effect as the stopper modification. Ammonia has previously been used to deprotonate TTA to improve the luminescence yield of ZL-based host–guest composites.[17,46] Ammonia escapes, however, quickly under ambient conditions and the improvement is therefore not sustainable. The luminescence intensity of Eu^{3+}('TTAn)-NZL-NH_3 decreases when kept under ambient conditions.

We conclude that all data clearly support the interpretation that the presence of stopper **1** is favorable to the formation of Eu^{3+}-β-diketonate complexes with large coordination number in a sustainable way by decreasing the proton strength inside of the channels of NZL. The main influence is caused by the stoppers directly bound to the channel entrance but also the molecules located on the coat seem to be of importance, probably by causing a slightly basic local environment. The large excess of **1** added to the reaction mixture is needed to plug as many of the channel entrances as possible in the adsorption equilibrium reaction step explained in Scheme 2.

A stable and semitransparent aqueous suspension can be obtained with NZL. We prepared suspensions with Eu^{3+}-(TTA_n)-NZL, $Eu^{3+}(TTA_n)$-NZL-NH_3, and $Eu^{3+}(TTA_n)$-NZL-**1**(1100). Only the suspension of the stopper-modified sample results in a bright emission upon irradiation at 345 nm (Supporting Information, Figure S5). This means that the stopper modification substantially prevents luminescence quenching of Eu^{3+} according to the mechanism explained above. Transparent films of a few micrometer thickness seen in Figure 5 A were obtained by dropping an aqueous suspension of $Eu^{3+}(TTA_n)$-NZL-**1**(1100) on the micro-slide glass, followed by drying at 60 °C in air. They exhibit bright red emission when irradiated by near UV light (Figure 5 B).

SEM images of the films show that the NZL (30–100 nm) are well-packed on the surface of the glass (Figure 5 C,D). The excitation and emission spectra of the film shown in Figure 5 E,F are similar to those seen in Figure 1. A broad band ranging from 200 to 400 nm forms the excitation spectrum. It can be attributed to the absorption of the TTA

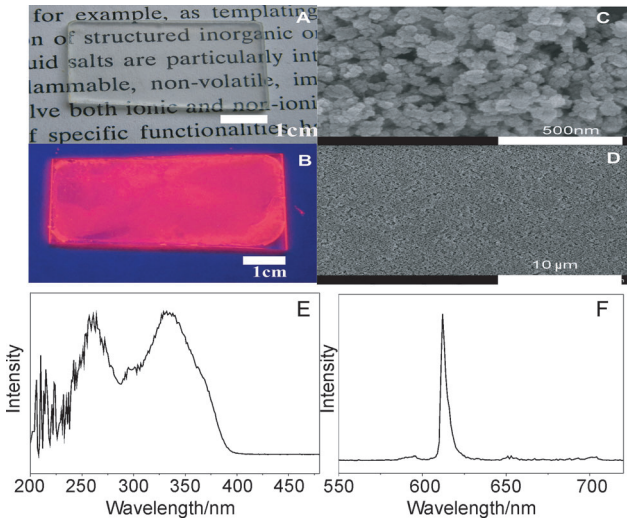

Figure 5. Properties of the $Eu^{3+}(TTA_n)$-NZL-**1**(1100) films. Images: daylight (A), UV light (B). SEM images at two magnifications (C, D). Spectra: excitation (E), monitored at 612 nm, and emission (F), excited at 345 nm.

ligand. Excitation at 345 nm results in the same $^5D_0 \rightarrow {}^7F_J$ emission lines as seen in Figure 1 with the $^5D_0 \rightarrow {}^7F_2$ band as the most intense feature. The intensity ratio $I(^5D_0 \rightarrow {}^7F_2)/I(^5D_0 \rightarrow {}^7F_1)$ is 18.7. The luminescence decay is bi-exponential (Supporting Information, Figure S6). The data in Table 1 shows that luminescence lifetime and q of the film are smaller than those of the $Eu^{3+}(TTA_n)$-NZL-**1**(1100) powder, which is due to less-favorable conditions during the film preparation. The thin film preparation procedures can be adapted and optimized for obtaining the desired properties depending on the envisaged application.

In conclusion, we have observed a remarkable increase of the luminescence efficiency of a host–guest composite, obtained by synthesizing Eu^{3+}-β-diketonate complexes inside of the channels of NZL using Lundford's ship-in-a-bottle procedure,[47] after modification with an imidazolium-based stopper molecule.[48] Our result is especially surprising and important when confronted with earlier reports regarding Eu^{3+}-β-diketonate complexes encapsulated within zeolites.[11,15,17] The mechanism responsible has been elucidated by comparing two different diketonate ligands with different pK_a values and two aromatic imines, BPY and PHEN, and by applying stationary and time-resolved spectroscopy. We found that all of the data support the interpretation that the presence of **1** is favorable to the sustainable formation of Eu^{3+}-β-diketonate complexes with high coordination numbers by decreasing the proton strength inside of the channels of NZL, the main influence being exerted by the stoppers directly bound to the channel entrance. A consequence of our finding is that strongly luminescent transparent films can be prepared using aqueous suspension. Properties of the new composites and films with respect to their utilization for sensing and optoelectronic devices are the topic of further investigations.

Received: December 3, 2013
Revised: December 30, 2013
Published online: February 6, 2014

Keywords: luminescence · rare earth elements · supramolecular chemistry · thin films · zeolites

[1] S. V. Eliseeva, J.-C. G. Bünzli, *Chem. Soc. Rev.* **2010**, *39*, 189–227.
[2] J. Graffion, X. Cattoën, M. Wong Chi Man, V. R. Fernandes, P. S. André, R. A. S. Ferreira, L. D. Carlos, *Chem. Mater.* **2011**, *23*, 4773–4782.
[3] L. Armelao, S. Quici, F. Barigelletti, G. Accorsi, G. Bottaro, M. Cavazzini, E. Tondello, *Coord. Chem. Rev.* **2010**, *254*, 487–505.
[4] O. Moudam, B. C. Rowan, M. Alamiry, P. Richardson, B. S. Richards, A. C. Jones, N. Robertson, *Chem. Commun.* **2009**, 6649–6651.
[5] J. Yu, L. Zhou, H. Zhang, Y. Zheng, H. Li, R. Deng, Z. Peng, Z. Li, *Inorg. Chem.* **2005**, *44*, 1611–1618.
[6] M. Shi, F. Li, T. Yi, D. Zhang, H. Hu, C. Huang, *Inorg. Chem.* **2005**, *44*, 8929–8936.
[7] L. Maggini, H. Traboulsi, K. Yoosaf, J. Mohanraj, J. Wouters, O. Pietraszkiewicz, M. Pietraszkiewicz, N. Armaroli, D. Bonifazi, *Chem. Commun.* **2011**, *47*, 1625–1627.
[8] L. D. Carlos, R. A. S. Ferreira, V. de Zea Bermudez, B. Julián-López, P. Escribano, *Chem. Soc. Rev.* **2011**, *40*, 536–549.
[9] K. Binnemans, *Chem. Rev.* **2009**, *109*, 4283–4374.
[10] H. Maas, A. Currao, G. Calzaferri, *Angew. Chem.* **2002**, *114*, 2607–2608; *Angew. Chem. Int. Ed.* **2002**, *41*, 2495–2497.
[11] D. Sendor, U. Kynast, *Adv. Mater.* **2002**, *14*, 1570–1574.
[12] M. Alvaro, V. Fornés, S. García, H. García, J. C. Scaiano, *J. Phys. Chem. B* **1998**, *102*, 8744–8750.
[13] Y. Wada, T. Okubo, M. Ryo, T. Nakazawa, Y. Hasegawa, S. Yanagida, *J. Am. Chem. Soc.* **2000**, *122*, 8583–8584.
[14] Y. Wada, M. Sato, Y. Tsukahara, *Angew. Chem.* **2006**, *118*, 1959–1962; *Angew. Chem. Int. Ed.* **2006**, *45*, 1925–1928.
[15] H. Li, W. Cheng, Y. Wang, B. Liu, W. Zhang, H. Zhang, *Chem. Eur. J.* **2010**, *16*, 2125–2130.
[16] Y. Wang, H. Li, L. Gu, Q. Gan, Y. Li, G. Calzaferri, *Microporous Mesoporous Mater.* **2009**, *121*, 1–6.
[17] Y. Ding, Y. Wang, H. Li, Z. Duan, H. Zhang, Y. Zheng, *J. Mater. Chem.* **2011**, *21*, 14755–14759.
[18] Y. Ding, Y. Wang, Y. Li, P. Cao, T. Ren, *Photochem. Photobiol. Sci.* **2011**, *10*, 543–547.
[19] Y. Wang, H. Li, W. Zhang, B. Liu, *Mater. Lett.* **2008**, *62*, 3167–3170.
[20] A. Monguzzi, G. Macchi, F. Meinardi, R. Tubino, M. Burger, G. Calzaferri, *Appl. Phys. Lett.* **2008**, *92*, 123301–123303.
[21] A. Mech, A. Monguzzi, F. Meinardi, J. Mezyk, G. Macchi, R. Tubino, *J. Am. Chem. Soc.* **2010**, *132*, 4574–4576.
[22] P. Cao, H. Li, P. Zhang, G. A. Calzaferri, *Langmuir* **2011**, *27*, 12614–12620.
[23] Y. Wang, H. Li, Y. Feng, H. Zhang, G. Calzaferri, T. Ren, *Angew. Chem.* **2010**, *122*, 1476–1480; *Angew. Chem. Int. Ed.* **2010**, *49*, 1434–1438.
[24] V. Valtchev, L. Tosheva, *Chem. Rev.* **2013**, *113*, 6734–6760.
[25] Z. J. Li, S. Li, H. M. Luo, Y. S. Yan, *Adv. Funct. Mater.* **2004**, *14*, 1019–1024.
[26] J. Kobler, H. Abrevaya, S. Mintova, T. Bein, *J. Phys. Chem. C* **2008**, *112*, 14274–14280.
[27] L. Tosheva, V. P. Valtchev, *Chem. Mater.* **2005**, *17*, 2494–2513.
[28] M. Tsapatsis, M. Lovallo, T. Okubo, M. E. Davis, M. Sadakata, *Chem. Mater.* **1995**, *7*, 1734–1741.
[29] S. Suárez, A. Devaux, J. Bañuelos, O. Bossart, A. Kunzmann, G. Calzaferri, *Adv. Funct. Mater.* **2007**, *17*, 2298–2306.

[30] H. Li, Y. Ding, P. Cao, H. Liu, Y. Zheng, *J. Mater. Chem.* **2012**, *22*, 4056 – 4059.
[31] H. Maas, G. Calzaferri, *Angew. Chem.* **2002**, *114*, 2389 – 2392; *Angew. Chem. Int. Ed.* **2002**, *41*, 2284 – 2288.
[32] G. Calzaferri, *Langmuir* **2012**, *28*, 6216 – 6231.
[33] D. Brühwiler, G. Calzaferri, T. Torres, J. H. Ramm, N. Gartmann, L.-Q. Dieu, I. López-Duarte, M. V. Martínez-Díaz, *J. Mater. Chem.* **2009**, *19*, 8040 – 8067.
[34] J. M. Beierle, R. Roswanda, P. M. Erne, A. C. Coleman, W. R. Browne, B. L. Feringa, *Part. Part. Syst. Charact.* **2013**, *30*, 273 – 279; B. Schulte, M. Tsotsalas, M. Becker, A. Studer, L. De Cola, *Angew. Chem.* **2010**, *122*, 7033 – 7036; *Angew. Chem. Int. Ed.* **2010**, *49*, 6881 – 6884.
[35] Z. Popović, M. Otter, G. Calzaferri, L. De Cola, *Angew. Chem.* **2007**, *119*, 6301 – 6304; *Angew. Chem. Int. Ed.* **2007**, *46*, 6188 – 6191.
[36] G. Calzaferri, S. Huber, H. Maas, C. Minkowski, *Angew. Chem.* **2003**, *115*, 3860 – 3888; *Angew. Chem. Int. Ed.* **2003**, *42*, 3732 – 3758.
[37] T. Ban, D. Brühwiler, G. Calzaferri, *J. Phys. Chem. B* **2004**, *108*, 16348 – 16352.
[38] M. Tsotsalas, K. Kopka, G. Luppi, S. Wagner, M. P. Law, M. Schäfers, L. De Cola, *ACS Nano* **2010**, *4*, 342 – 348.
[39] D. P. Fasce, R. J. J. Williams, L. Matějka, J. Pleštil, J. Brus, B. Serrano, J. C. Cabanelas, J. Baselga, *Macromolecules* **2006**, *39*, 3794 – 3801.
[40] B. Hennessy, S. Megelski, C. Marcolli, V. Shklover, C. Bärlocher, G. Calzaferri, *J. Phys. Chem. B* **1999**, *103*, 3340 – 3351.
[41] A. Z. Ruiz, D. Brühwiler, T. Ban, G. Calzaferri, *Monatsh. Chem.* **2005**, *136*, 77 – 89; S. Megelski, G. Calzaferri, *Adv. Funct. Mater.* **2001**, *11*, 277 – 286.
[42] R. Q. Albuquerque, G. Calzaferri, *Chem. Eur. J.* **2007**, *13*, 8939 – 8952.
[43] M. Klähn, A. Seduraman, P. Wu, *J. Phys. Chem. B* **2011**, *115*, 8231 – 8241.
[44] S. Tang, A. Babai, A.-V. Mudring, *Angew. Chem.* **2008**, *120*, 7743 – 7746; *Angew. Chem. Int. Ed.* **2008**, *47*, 7631 – 7634.
[45] M. Fernandes, V. de Zea Bermudez, R. A. Sá Ferreira, L. D. Carlos, A. Charas, J. Morgado, M. M. Silva, M. J. Smith, *Chem. Mater.* **2007**, *19*, 3892 – 3901.
[46] T. Wen, W. Zhang, X. Hu, L. He, H. Li, *ChemPlusChem* **2013**, *78*, 438 – 442.
[47] W. DeWilde, G. Peeters, J. H. Lunsford, *J. Phys. Chem.* **1980**, *84*, 2306 – 2310.
[48] Y. Lu, S. S. Moganty, J. L. Schaefer, L. A. Archer, *J. Mater. Chem.* **2012**, *22*, 4066 – 4072.

